with the O1–O2–C53 plane (102.3°). The staggering of the axial ligands indicated by these dihedral angles may prevent severe nonbonded contacts with the porphyrin core.

Comparison of $OTeF_5^-$ to Other Anionic Ligands. A cyclic voltammogram (CV) background scan of $[N(n\text{-}Bu)_4^+][OTeF_5^-]$ in dichloromethane was essentially flat from +2.5 to −1.5 V (SCE). When $Fe(TPP)(ClO_4)$ was added to this solution, the CV showed an irreversible reduction at −0.16 V (Fe(III)/Fe(II)). Since the reduction of $Fe(TPP)(ClO_4)$ has been reported to occur at +0.14[55] and +0.22 V[56] in dichloromethane containing 0.10 M $[N(n\text{-}Bu)_4^+][ClO_4^-]$, replacement of ClO_4^- by $OTeF_5^-$ must have occurred. CV's of $Fe(TPP)(OTeF_5)$ in 0.1 M $[N(n\text{-}Bu)_4^+][OTeF_5^-]$ were measured in dichloromethane and showed the same irreversible reduction at −0.16 V. Since the −0.16-V value is anodic of the values found for high-spin Fe(III) halides[56] but cathodic of those for ClO_4^- and $CF_3SO_3^-$[31c] complexes, teflate lies between the halides and the weak ligands perchlorate and triflate in ligand-binding character.[56] The first oxidation of $Fe(TPP)(OTeF_5)$ appears as a quasi-reversible wave with a half-wave potential of 1.01 V. This value compares favorably with the half-wave potentials of 1.08–1.11 V found for the first oxidation of five-coordinate Fe(III) porphyrins.[55,57] The cathodic value of the potential is indicative of ring oxidation instead of metal-centered oxidation (cf. $Fe(TPP)F_2^-$, $E_{1/2}$ = 0.68 V for Fe(III)/Fe(IV)[58]).

Ligand displacement reactions were investigated by solution infrared spectroscopy to further confirm the ligand-binding strength of teflate relative to that of chloride and perchlorate. When 1 equiv of $N(n\text{-}Bu)_4^+Cl^-$ was added to a dichloromethane solution of $Fe(TPP)(OTeF_5)$, the complete displacement of teflate by chloride was indicated by the disappearance of the 848-cm^{-1} ν(TeO) band and the appearance of an 861-cm^{-1} band for the TeO stretch of free, ionic teflate.[12] Likewise, the complete displacement of ClO_4^- by $OTeF_5^-$ upon addition of $[N(n\text{-}Bu)_4^+][OTeF_5^-]$ to a dichloromethane solution of $Fe(TPP)(ClO_4)$ was shown by the disappearance of the 861-cm^{-1} band for free teflate and the appearance of ν(TeO) at 848-cm^{-1} for $Fe(TPP)(OTeF_5)$ and a free perchlorate band at 624-cm^{-1} (asymmetric bend).[59] Since it is known that Cl^- will displace ClO_4^- in $Fe(Por)(ClO_4)$ complexes,[60] the ligand displacement reactions confirm the ligand-binding strengths found electrochemically, $Cl^- > OTeF_5^- > ClO_4^-$.

Summary and Conclusions. This study has shown that $OTeF_5^-$ forms high-spin $Fe(Por)(OTeF_5)$ and $Fe(TPP)(OTeF_5)(THF)$ complexes. The iron–teflate bonds are moderately strong with a large component of ionic character, and the ligand binding strength of teflate follows the order $Cl^- > OTeF_5^- > ClO_4^-$. The electronic and steric differences between teflate and other weakly basic oxyanions such as perchlorate and triflate suggest that teflate may be a useful ligand for highly reactive complexes, where a small change in ligand properties can produce dramatic differences in reactivity.

Acknowledgment. This research was supported by grants from the National Science Foundation (CHE-8419719) and the National Institutes of Health (GM 31554). We thank Professor J. R. Norton for the use of his IR spectrometer and J. H. Reibenspies and M. M. Miller for experimental assistance. P.J.K. thanks the Mobay Corp. for a Graduate Student Research Award. The Nicolet R3m/E diffractometer and computing system was purchased with a grant from the NSF (CHE-8103011).

Registry No. $[AgOTeF_5(CH_3CN)_2]_2$, 98330-70-2; $[Fe(TPP)]_2O$, 12582-61-5; $[Fe(OEP)]_2O$, 39393-88-9; $Fe(TPP)(ClO_4)$, 59370-87-5; $Fe(TPP)(OTeF_5)$, 113704-01-1; $Fe(TPP)(^{18}OTeF_5)$, 118207-88-8; $Fe(OEP)(OTeF_5)$, 113704-02-2; $Fe(OEP)(^{18}OTeF_5)$, 118207-89-9; $Fe(TPP)(OTeF_5)(THF)$, 118207-90-2; Fe(TPP)Cl, 16456-81-8.

Supplementary Material Available: Numbering scheme of the $Fe(TPP)^+$ moiety of $Fe(TPP)(OTeF_5)(THF)$ (Figure S1), a complete listing of the details of the X-ray crystallographic experiment (Table S-I), a complete listing of interatomic distances and angles (Table S-II), a listing of anisotropic thermal parameters for all non-hydrogen atoms (Table S-III), a table of hydrogen atom positions and isotropic thermal parameters (Table S-IV), and a table of linear least-squares parameters for δ versus $1/T$ plots for $Fe(TPP)(OTeF_5)$ and $Fe(OEP)(OTeF_5)$ (Table S-VI) (13 pages); a table of observed and calculated structure factors (Table S-V) (25 pages). Ordering information is given on any current masthead page.

(55) Phillippi, M. A.; Shimomura, E. T.; Goff, H. M. *Inorg. Chem.* **1981**, *20*, 1322.
(56) Bottomley, L. A.; Kadish, K. M. *Inorg. Chem.* **1981**, *20*, 1348.
(57) Kadish, K. M.; Bottomley, L. A. *Inorg. Chem.* **1980**, *19*, 832.
(58) Hickman, D. L.; Goff, H. M. *Inorg. Chem.* **1983**, *22*, 2789.
(59) Gowda, N. M. N.; Naikar, S. B.; Reddy, G. K. N. *Adv. Inorg. Chem. Radiochem.* **1984**, *28*, 255.
(60) In ref 57, Kadish et al. calculated K_{ex} = 10.3 for the reaction $Fe(TPP)(ClO_4) + Cl^- \rightleftharpoons Fe(TPP)Cl + ClO_4^-$; however, no $Fe(OEP)(ClO_4)$ was detected by cyclic voltammetry in the reaction of $Fe(OEP)(ClO_4)$ with 1 equiv of Cl^-.

Contribution from the Department of Chemistry, Faculty of Science, Tohoku University, Aoba, Aramaki, Sendai 980, Japan

(μ-Ethylenediaminetetraacetato)(μ-oxo)(μ-sulfido)bis(oxotungstate(V)): The First Crystallographically Characterized Complex Containing the $W_2(O)_2(\mu\text{-}O)(\mu\text{-}S)$ Unit

Shinji Ikari, Yoichi Sasaki,* and Tasuku Ito*

Received July 13, 1988

Neutralization by aqueous 2 M Na_2CO_3 of an H_2S-saturated aqueous solution of $(NH_4)_2[WOCl_5]$ and disodium dihydrogen ethylenediaminetetraacetate (Na_2H_2edta) gave a mixture of the title complex and the known $[W_2(O)_2(\mu\text{-}O)_2(\mu\text{-edta})]^{2-}$. The new complex was purified by the use of an anion-exchange column (QAE-Sephadex A-25). The crystal of $Ba[W_2(O)_2(\mu\text{-}O)(\mu\text{-}S)(\mu\text{-edta})]\cdot 6.5H_2O$ ($W_2BaSO_{17.5}N_2C_{10}H_{25}$) is orthorhombic, space group *Fdd*2, with a = 25.323 (1) Å, b = 50.706 (5) Å, c = 7.077 (1) Å, V = 9087.5 (4) Å^3, and Z = 16. The structure was solved by using 4075 unique reflections with $|F_o| > 3\sigma(F_o)$ to give R = 0.034. The metal-to-metal distance is 2.654 (1) Å, which is in the range of a direct metal–metal bond. Bond distances and angles within the $W_2(O)_2(\mu\text{-}O)(\mu\text{-}S)$ moiety are very similar to those of the known $Mo_2(O)_2(\mu\text{-}O)(\mu\text{-}S)$ unit. $[W_2(O)_2(\mu\text{-}O)(\mu\text{-}S)(\mu\text{-edta})]^{2-}$ exhibits absorption peaks at 440 nm (ϵ = 240 M^{-1} cm^{-1}) and 273 (9430) in water. Cyclic voltammetry in aqueous solution (pH 7.5, 0.2 M phosphate buffer) shows one irreversible oxidation wave at +0.65 V vs SCE with a glassy-carbon electrode. ^1H and ^{13}C NMR spectra in D_2O are consistent with the rapid inversion of the pseudo-gauche structure of the N–C–C–N bridge. The XPS spectrum in the solid state indicates binding energies of the metal 4d and 4f electrons lower than those of $[W_2(O)_2(\mu\text{-}O)_2(\mu\text{-edta})]^{2-}$.

Introduction

Molybdenum(V) is known to form preferably dimeric complexes with the $Mo_2(O)_2(\mu\text{-}O)_2$ core in aqueous media. All the bridging and terminal oxide ions can successively be replaced by sulfide ions, and the following cores are now known: $Mo_2(O)_2(\mu\text{-}O)(\mu\text{-}S)$, $Mo_2(O)_2(\mu\text{-}S)_2$, $Mo_2(O)(S)(\mu\text{-}S)_2$, and $Mo_2(S)_2(\mu\text{-}S)_2$.[1] Tung-

0020-1669/89/1328-0447$01.50/0

sten(V) also forms complexes with the $W_2(O)_2(\mu\text{-}O)_2$ core, and the X-ray crystal structures of the F^{-2} and the edta^{4-} (ethylenediaminetetraacetate(4−))[3] complexes have been determined. The complexes with $W_2(O)_2(\mu\text{-}S)_2$ cores, i.e. $W_2(O)_2(\mu\text{-}S)_2Cl_4$,[4] $[W_2(O)_2(\mu\text{-}S)_2(S_4)_2]^{2-}$,[5] and $[W_2(O)_2(\mu\text{-}S)_2(cys)_2]^{2-}$ (cys = (*R*)-cysteinate(2−)),[6] and those with $W_2(S)_2(\mu\text{-}S)_2$ cores, i.e. $W_2(S)_2(\mu\text{-}S)_2(WS_4)_2$,[7] $[W_2(S)_2(\mu\text{-}S)_2(S_4)_2]^{2-}$,[5,8] $[W_2(S)_2(\mu\text{-}S)_2(S_2)(S_4)]^{2-}$,[5] $W_2(S)_2(\mu\text{-}S)_2(S_2C_2H_4)_2$,[9] and $W_2(S)_2(\mu\text{-}S)_2[S_2P(OC_2H_5)_2]_2$,[10] have also been analyzed by X-ray crystallography. No X-ray crystal structure determination has so far been reported for a complex with the $W_2(O)_2(\mu\text{-}O)(\mu\text{-}S)$ core, although complexes with this core were claimed to be prepared with dithiocarbamate ligands.[11]

We have been preparing unknown members of the series of edta complexes $[MM'(O)_2(\mu\text{-}X)(\mu\text{-}Y)(\mu\text{-edta})]^{2-}$ (M, M' = Mo, W; X, Y = O, S) in order to study various properties of this type of complex in a systematic way. We reported recently the mixed-metal complex $[MoW(O)_2(\mu\text{-}O)_2(\mu\text{-edta})]^{2-}$.[12,13] This paper reports a new complex, $[W_2(O)_2(\mu\text{-}O)(\mu\text{-}S)(\mu\text{-edta})]^{2-}$, which provides the first example of a complex with the $W_2(O)_2(\mu\text{-}O)(\mu\text{-}S)$ core whose crystal structure has been determined. Various properties of the new ditungsten(V) complex are compared with those of the corresponding molybdenum(V) complexes and of the $W_2(O)_2(\mu\text{-}O)_2$ and $W_2(O)_2(\mu\text{-}S)_2$ complexes.

Experimental Section

1. Preparation of the Complexes. (a) Disodium (μ-Ethylenediaminetetraacetato)(μ-oxo)(μ-sulfido)bis(oxotungstate(V)), $Na_2[W_2(O)_2(\mu\text{-}O)(\mu\text{-}S)(\mu\text{-edta})]$. $(NH_4)_2[WOCl_5]$[14] (20 g, 0.048 mol) was added to an H_2S-saturated aqueous solution (250 cm^3) of 18 g (0.048 mol) of disodium dihydrogen ethylenediaminetetraacetate dihydrate. The solution was slowly neutralized with aqueous 2 M Na_2CO_3 solution. Nitrogen gas was passed through the solution to remove excessive H_2S, and the solution was filtered. The filtrate was then diluted with a large amount of water and poured onto an anion-exchange column of QAE-Sephadex A-25 (5 cm in diameter and 30 cm in length). The column was washed with water and then connected to two columns (3 cm in diameter and 80 cm in length) containing the same resin. On elution with 0.15 M $NaClO_4$ solution, the brown band of the μ-oxo-μ-sulfido complex was obtained separately, after 3 weeks, from the preceding yellow band of the bis(μ-oxo)ditungsten(V) complex. The brown eluate was concentrated and filtered to remove $NaClO_4$. Ethanol was added to the filtrate, and the solution was cooled in a refrigerator to obtain orange crystals. They were collected by filtration, washed with ethanol, and then dried in vacuo; yield 2.3 g (12%). These were recrystallized from water by adding ethanol. Anal. Calcd for $C_{10}H_{12}N_2O_{11}SNa_2W_2$: C, 15.36; H, 1.55; N, 3.58; S, 4.10. Found: C, 15.47; H, 2.65; N, 3.67; S, 3.67. IR (cm^{-1}): 3578 sh, 3420 br, 1648 s, 1450 w, 1396 s, 1365 sh, 1350 sh, 1236 w, 949 s, 929 m, 907 m, 874 m, 745 m, 558 w, 481 m, 443 w, 415 w.

Table I. Crystallographic Data and Details of the Structure Determination for $Ba[W_2(O)_2(\mu\text{-}O)(\mu\text{-}S)(\mu\text{-edta})]\cdot 6.5H_2O$

chem formula: $W_2BaSO_{17.5}N_2C_{10}H_{25}$	fw = 990.41
a = 25.323 (1) Å	orthorhombic space group: *Fdd*2 (No. 43)
b = 50.706 (5) Å	T = 13 °C
c = 7.077 (1) Å	λ = 0.71069 Å
V = 9087.5 (4) Å^3	ρ_{obsd} = 2.95 g cm^{-3}
Z = 16	ρ_{calcd} = 2.90 g cm^{-3}
$F(000)$ = 7344	μ = 126.48 cm^{-1}

systematic absences: hkl, $(h + k, k + l) \neq 2n$; $0kl$, $h + k \neq 4n$; $h0l$, $l + h \neq 4n$
cryst size: 0.15 × 0.08 × 0.25 mm
rflns measd: $+h,+k,+l$
2θ range: 3–65°
scan type: 2θ–ω
scan range: $(1.4 + 0.3 \tan \theta)°$
scan speed (θ): 4.0° min^{-1}
no. of measd data: 4586
no. of unique data ($|F_o| > 3\sigma(F_o)$): 4075
no. of params: 308
R = 0.0343[a]
R_w = 0.0344[b]
GOF = 2.26[c]

[a] $R = \sum||F_o| - |F_c||/\sum|F_o|$. [b] $R_w = [\sum w(|F_o| - |F_c|)^2/\sum|F_o|^2]^{1/2}$, $w = 1/\sigma^2(|F_o|)$. [c] GOF = $[\sum w(|F_o| - |F_c|)^2/(N_o - N_p)]^{1/2}$, where N_o and N_p are the numbers of observations and parameters, respectively.

The barium salt $Ba[W_2(O)_2(\mu\text{-}O)(\mu\text{-}S)(\mu\text{-edta})]\cdot 6.5H_2O$ was prepared by adding a saturated $BaCl_2$ solution to an aqueous solution of the sodium salt.

(b) Other Complexes. $Na_2[W_2(O)_2(\mu\text{-}O)_2(\mu\text{-edta})]\cdot 3H_2O$ was prepared by the method in the literature[15] and purified by the use of anion-exchange chromatography (QAE-Sephadex A-25). $Na_2[Mo_2(O)_2(\mu\text{-}O)_2(\mu\text{-edta})]$[16] was prepared from $Na_2[Mo_2(O)_2(\mu\text{-}O)_2(C_2O_4)_2(H_2O)_2]$[17] by a method similar to that for the $W_2(O)_2(\mu\text{-}O)_2$ complex. $Na_2[Mo_2(O)_2(\mu\text{-}O)(\mu\text{-}S)(\mu\text{-edta})]\cdot 2H_2O$[18] was obtained as a byproduct in the preparation of a new mixed-metal complex, $Na_2[MoW(O)_2(\mu\text{-}O)(\mu\text{-}S)(\mu\text{-edta})]$.[19] $Na_2[Mo_2(O)_2(\mu\text{-}S)_2(\mu\text{-edta})]$[18] and $Na_2[W_2(O)_2(\mu\text{-}S)_2(\mu\text{-edta})]$[20] were prepared by using the reported methods.

2. Measurements. Ultraviolet and visible absorption spectra were measured with a Hitachi 330 and Hitachi 340 spectrophotometers. Infrared absorption spectra were measured by a Jasco IR-810 spectrophotometer with KBr pellets at room temperature. X-ray photoelectron spectra were obtained by a VG-ESCA LAB Mark II instrument using Mg Kα exciting radiation at ambient temperature and at pressure less than 10^{-9} Torr. The energy scale was calibrated by emission from the C 1s (methylene carbon) line at 284.6 eV. Samples were prepared as thin films on Al metal by evaporating acetonitrile solutions. Electrochemical measurements were carried out in aqueous solutions by using a Yanaco P-1100 polarographic analyzer with a glassy-carbon working electrode at 24 ± 2 °C. Cyclic voltammograms were obtained at a scan rate of 20 mV/s, potentials being recorded vs SCE. The pH values of the solutions were fixed to 7.5 (special-grade reagents, $NaH_2PO_4\cdot 12H_2O$, $Na_2HPO_4\cdot 12H_2O$, and $Na_2SO_4\cdot 10H_2O$, were used to make buffer solutions after recrystallization from water). The concentration of the complex was 0.001 M. ^{1}H NMR spectra were measured on a JEOL GSX-270 FT-NMR spectrometer at 270 MHz and 80 °C. ^{13}C NMR spectra were measured on a Varian XL-200 FT-NMR spectrometer at 50.2 MHz and 28 ± 1 °C.

3. Crystal Structure Determination. Crystals of the barium salt for the X-ray structure determination were obtained by slow crystallization from the aqueous solution by adding ethanol. They are air-stable. A crystal (0.15 × 0.08 × 0.25 mm) of the barium salt was attached to the end of a glass fiber and mounted on a Rigaku AFC-5R four-circle diffractometer equipped with a rotating anode (40 kV, 200 mV). Crystallographic data and data collection parameters are summarized in

(1) Cotton, F. A.; Wilkinson, G. *Advanced Inorganic Chemistry*, 5th ed.; Wiley: New York, 1988; p 831.
(2) Mattes, R.; Mennemann, K. *Z. Anorg. Allg. Chem.* **1977**, *437*, 175–182.
(3) (a) Khalil, S.; Sheldrick, B.; Soares, A. B.; Sykes, A. G. *Inorg. Chim. Acta* **1977**, *25*, L83–L84. (b) Khalil, S.; Sheldrick, B. *Acta Crystallogr., Sect. B: Struct. Crystallogr. Cryst. Chem.* **1978**, *B34*, 3751–3753.
(4) Drew, M. G. B.; Page, E. M.; Rice, D. A. *Inorg. Chim. Acta* **1983**, *76*, L33–L34.
(5) Müller, A.; Romer, M.; Romer, C.; Reinsch-Vogell, U.; Bogger, H.; Schimanski, U. *Monatsh. Chem.* **1985**, *116*, 711–715.
(6) Shibahara, T.; Izumori, Y.; Kubota, R.; Kuroya, H. *Chem. Lett.* **1987**, 2327–2330.
(7) Secheresse, F.; Lefebvre, J.; Daran, J. C.; Jeannin, Y. *Inorg. Chem.* **1982**, *21*, 1311–1314.
(8) Cohen, S. A.; Stiefel, E. I. *Inorg. Chem.* **1985**, *24*, 4657–4662.
(9) Pan, W.-H.; Chandler, T.; Enemark, J. H.; Stiefel, E. I. *Inorg. Chem.* **1984**, *23*, 4265–4269.
(10) Drew, M. G. B.; Hobson, R. J.; Mumba, P. P. E. M.; Rice, D. A.; Turp, N. *J. Chem. Soc., Dalton Trans.* **1987**, 1163–1167.
(11) (a) Lozano, R.; Alarcon, E.; Doadrio, A. L.; Doadrio, A. *Polyhedron* **1983**, *2*, 435–441; **1984**, *3*, 25–29; *An. Quim., Ser. B* **1983**, *79*, 37–40, (b) Lozano, R.; Doadrio, A. L.; Alarcon, E.; Roman, J.; Doadrio, A. *Rev. Chim. Miner.* **1983**, *20*, 109–117.
(12) Wang, B.; Sasaki, Y.; Ikari, S.; Kimura, K.; Ito, T. *Chem. Lett.* **1987**, 1955–1958.
(13) Ikari, S.; Sasaki, Y.; Nagasawa, A.; Kabuto, C.; Ito, T. *Inorg. Chem.*, submitted for publication.
(14) Collenberg, O. *Z. Anorg. Allg. Chem.* **1918**, *102*, 247–276.
(15) Novak, J.; Podlaha, J. *J. Inorg. Nucl. Chem.* **1974**, *36*, 1061–1065.
(16) Pecsok, R. L.; Sawyer, D. T. *J. Am. Chem. Soc.* **1956**, *78*, 5496–5500.
(17) Cotton, F. A.; Morehouse, S. M. *Inorg. Chem.* **1965**, *4*, 1377–1381.
(18) Ott, V. R.; Swieter, D. S.; Schultz, F. A. *Inorg. Chem.* **1977**, *16*, 2538–2545.
(19) The complex $Na_2[MoW(O)_2(\mu\text{-}O)(\mu\text{-}S)(\mu\text{-edta})]\cdot 3H_2O$ will be reported elsewhere (Ikari, S.; Sasaki, Y.; Ito, T. Work in progress).
(20) Shibahara, T.; Izumori, Y.; Kubota, R.; Taniguchi, Y.; Kuroya, H. Presented at the 37th National Conference on Coordination Chemistry, Tokyo, Oct 1987; see Abstract 1AP06.

Table II. Positional and Equivalent Isotropic Thermal Parameters for $Ba[W_2(O)_2(\mu\text{-}O)(\mu\text{-}S)(\mu\text{-edta})]\cdot 6.5H_2O$[a]

atom	x	y	z	B_{eq}, Å^2
W(1)	4695 (2)	13175 (1)	-4214 (8)	1.2
W(2)	3877 (2)	7991 (1)	0	1.2
Ba	16474 (3)	644 (1)	-7470 (12)	1.7
S	-2538 (11)	11028 (5)	9841 (43)	1.6
O(1)	8946 (35)	13890 (17)	15291 (133)	2.0
O(2)	761 (35)	16824 (16)	13 (147)	2.2
O(3)	8859 (35)	15476 (18)	-22136 (144)	2.4
O(4)	-4094 (42)	20092 (17)	-10805 (169)	2.8
O(5)	9072 (49)	18121 (22)	-46329 (168)	3.7
O(6)	7747 (34)	7570 (16)	21058 (137)	2.0
O(7)	7905 (34)	4855 (16)	-12313 (153)	2.2
O(8)	-1444 (34)	5015 (17)	8158 (146)	2.1
O(9)	7580 (39)	1279 (17)	-30026 (177)	2.9
O(10)	-8859 (41)	2803 (19)	3939 (171)	3.0
O(11)	7846 (35)	10206 (16)	-16350 (124)	1.8
N(1)	-1028 (34)	13726 (17)	-30563 (143)	1.4
N(2)	-1342 (36)	6906 (16)	-26443 (140)	1.5
C(1)	-2593 (45)	17771 (20)	-11651 (183)	1.7
C(2)	-4903 (45)	15871 (20)	-25362 (196)	2.0
C(3)	7068 (49)	16276 (22)	-37715 (202)	2.1
C(4)	2436 (52)	14665 (26)	-46224 (182)	2.2
C(5)	5747 (46)	3412 (21)	-25132 (184)	1.8
C(6)	910 (51)	4508 (21)	-35484 (189)	2.0
C(7)	-5726 (47)	4501 (22)	-958 (210)	2.1
C(8)	-6657 (46)	6175 (24)	-18665 (209)	2.1
C(9)	-4507 (41)	11520 (20)	-37229 (167)	1.4
C(10)	-1799 (43)	8901 (20)	-42142 (168)	1.5
Ow(1)	20405 (39)	-4407 (17)	-879 (155)	2.6
Ow(2)	27000 (37)	-54 (18)	-20121 (163)	2.7
Ow(3)	14085 (43)	8512 (23)	-46333 (170)	3.3
Ow(4)	19268 (45)	4024 (20)	-34904 (187)	3.4
Ow(5)	38868 (44)	-1957 (21)	-22989 (183)	3.4
Ow(6)	34679 (55)	2223 (22)	3925 (212)	4.2
Ow(7)[b]	0	0	-71488 (251)	3.5

[a] The atomic numbering is shown in Figure 1. Positional parameters are multiplied by 10^5. [b] Ow(7) is at a special position.

Table I. Intensity data were obtained by using graphite-monochromated Mo Kα radiation and corrected for Lorentz and polarization factors. The absorption correction was made according to the method for a polyhedral model.[21] Atomic scattering factors, f_o, $\Delta f'$, and $\Delta f''$, were taken from ref 22.

The structures were solved by the heavy-atom method and refined by the block-diagonal least-squares method. The function used in the least-squares minimization was $\sum w[|F_o| - |F_c|]^2$, where $w = 1/\sigma^2(|F_o|)$. Anisotropic temperature factors were applied to all non-hydrogen atoms. The final refinement gave $R = 0.0343$. Hydrogen atoms were not included in the analysis. A final difference Fourier synthesis indicated no significant peaks of more than 1.0 e Å^{-3}.

All calculations were performed with the Universal Crystallographic Computer Program System, UNICS III[23] on an ACOS-1000 computer at the Computer Center of Tohoku University. Atomic positional parameters are given in Table II. Tables of the anisotropic thermal parameters (Table SI) and the structure factors (Table SII) are available as supplementary material.

Results and Discussion

1. Crystal and Molecular Structure of the Complex Anion. Figure 1 shows an ORTEP drawing of the complex anion $[W_2(O)_2(\mu\text{-}O)(\mu\text{-}S)(\mu\text{-edta})]^{2-}$ together with its numbering scheme. Bond distances and angles within the anion are summarized in Table III. The overall structure of the anion is very similar to those of the other edta complexes $[W_2(O)_2(\mu\text{-}O)_2(\mu\text{-edta})]^{2-}$,[3] $[Mo_2(O)_2(\mu\text{-}S)_2(\mu\text{-edta})]^{2-}$,[24] and $[MoW(O)_2(\mu\text{-}O)_2(\mu\text{-edta})]^{2-}$.[13] The N–C–C–N part of the edta ligand takes a distorted gauche

(21) Busing, W. R.; Levy, H. A. *Acta Crystallogr.* **1957**, *10*, 180–182. De Meulenaer, J.; Tompa, H. *Acta Crystallogr.* **1965**, *19*, 1014–1048.
(22) *International Tables for X-Ray Crystallography*; Kynoch: Birmingham, England, 1974; Vol. IV.
(23) Sakurai, T.; Kobayashi, K. *Sci. Rep. Inst. Chem. Phys. Res. (Jpn.)* **1979**, *55*, 69–77.
(24) Spivack, B.; Dori, Z. *J. Chem. Soc., Dalton Trans.* **1973**, 1173–1177.

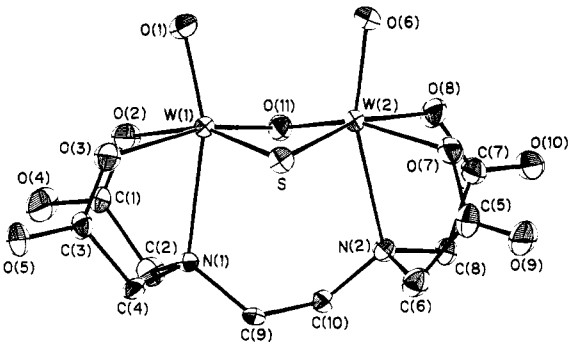

Figure 1. Structure of the $[W_2(O)_2(\mu\text{-}O)(\mu\text{-}S)(\mu\text{-edta})]^{2-}$ ion and its atomic numbering scheme. The thermal ellipsoids are drawn at 50% probability.

Table III. Interatomic Distances and Angles for $[W_2(O)_2(\mu\text{-}O)(\mu\text{-}S)(\mu\text{-edta})]^{2-}$

Bond Distances (Å)			
W(1)–W(2)	2.6536 (6)		
W(1)–S	2.352 (3)	W(2)–S	2.344 (3)
W(1)–O(1)	1.788 (9)	W(2)–O(6)	1.796 (9)
W(1)–O(2)	2.123 (8)	W(2)–O(7)	2.081 (9)
W(1)–O(3)	2.02 (1)	W(2)–O(8)	2.104 (9)
W(1)–O(11)	1.908 (8)	W(2)–O(11)	1.900 (9)
W(1)–N(1)	2.38 (1)	W(2)–N(2)	2.36 (1)
O(2)–C(1)	1.28 (2)	O(7)–C(5)	1.29 (2)
O(4)–C(1)	1.24 (1)	O(9)–C(5)	1.23 (1)
N(1)–C(2)	1.51 (1)	N(2)–C(6)	1.49 (1)
C(1)–C(2)	1.49 (2)	C(5)–C(6)	1.53 (2)
O(3)–C(3)	1.26 (2)	O(8)–C(7)	1.29 (2)
O(5)–C(3)	1.23 (2)	O(10)–C(7)	1.22 (2)
N(1)–C(4)	1.49 (2)	N(2)–C(8)	1.50 (2)
C(3)–C(4)	1.55 (2)	C(7)–C(8)	1.53 (2)
N(1)–C(9)	1.50 (1)	N(2)–C(10)	1.51 (1)
C(9)–C(10)	1.53 (1)		
Bond Angles (deg)			
W(2)–W(1)–S	55.46 (7)	W(1)–W(2)–S	55.72 (7)
W(2)–W(1)–O(1)	99.3 (3)	W(1)–W(2)–O(6)	99.7 (3)
W(2)–W(1)–O(2)	144.2 (2)	W(1)–W(2)–O(7)	132.2 (3)
W(2)–W(1)–O(3)	133.1 (3)	W(1)–W(2)–O(8)	142.3 (2)
W(2)–W(1)–O(11)	45.7 (3)	W(1)–W(2)–O(11)	46.0 (3)
W(2)–W(1)–N(1)	99.0 (2)	W(1)–W(2)–N(2)	100.7 (2)
S–W(1)–O(1)	103.7 (3)	S–W(2)–O(6)	102.1 (3)
S–W(1)–O(2)	88.8 (3)	S–W(2)–O(7)	165.1 (3)
S–W(1)–O(3)	160.0 (3)	S–W(2)–O(8)	86.9 (3)
S–W(1)–O(11)	98.7 (3)	S–W(2)–O(11)	99.2 (3)
S–W(1)–N(1)	84.9 (2)	S–W(2)–N(2)	90.0 (2)
O(1)–W(1)–O(2)	89.8 (4)	O(6)–W(2)–O(7)	89.4 (4)
O(1)–W(1)–O(3)	93.1 (4)	O(6)–W(2)–O(8)	92.1 (4)
O(1)–W(1)–O(11)	104.8 (4)	O(6)–W(2)–O(11)	106.7 (4)
O(1)–W(1)–N(1)	161.5 (3)	O(6)–W(2)–N(2)	159.6 (3)
O(2)–W(1)–O(3)	80.2 (4)	O(7)–W(2)–O(8)	83.2 (4)
O(2)–W(1)–O(11)	161.4 (4)	O(7)–W(2)–O(11)	86.4 (4)
O(2)–W(1)–N(1)	73.9 (3)	O(7)–W(2)–N(2)	76.3 (3)
O(3)–W(1)–O(11)	87.4 (4)	O(8)–W(2)–O(11)	158.4 (4)
O(3)–W(1)–N(1)	76.0 (3)	O(8)–W(2)–N(2)	72.0 (4)
O(11)–W(1)–N(1)	89.7 (3)	O(11)–W(2)–N(2)	87.2 (3)
W(1)–S–W(2)	68.82 (8)	W(1)–O(11)–W(2)	88.3 (4)
W(1)–O(2)–C(1)	123.3 (8)	W(2)–O(7)–C(5)	121.4 (8)
W(1)–N(1)–C(2)	106.8 (7)	W(2)–N(2)–C(6)	108.5 (7)
O(2)–C(1)–O(4)	122.0 (12)	O(7)–C(5)–O(9)	122.6 (11)
O(2)–C(1)–C(2)	116.1 (9)	O(7)–C(5)–C(6)	118.1 (10)
O(4)–C(1)–C(2)	121.8 (11)	O(9)–C(5)–C(6)	119.2 (11)
N(1)–C(2)–C(1)	111.7 (9)	N(2)–C(6)–C(5)	113.4 (10)
W(1)–O(3)–C(3)	123.2 (8)	W(2)–O(8)–C(7)	123.1 (8)
W(1)–N(1)–C(4)	105.2 (7)	W(2)–N(2)–C(8)	105.6 (7)
O(3)–C(3)–O(5)	122.1 (12)	O(8)–C(7)–O(10)	123.2 (13)
O(3)–C(3)–C(4)	116.3 (11)	O(8)–C(7)–C(8)	115.3 (10)
O(5)–C(3)–C(4)	121.4 (13)	O(10)–C(7)–C(8)	121.5 (12)
N(1)–C(4)–C(3)	108.9 (10)	N(2)–C(8)–C(7)	107.4 (9)
C(2)–N(1)–C(4)	109.5 (9)	C(6)–N(2)–C(8)	107.4 (9)
W(1)–N(1)–C(9)	121.1 (7)	W(2)–N(2)–C(10)	118.2 (6)
C(2)–N(1)–C(9)	103.4 (8)	C(6)–N(2)–C(10)	105.1 (9)
C(4)–N(1)–C(9)	110.5 (9)	C(8)–N(2)–C(10)	111.6 (9)
N(1)–C(9)–C(10)	117.0 (9)	N(2)–C(10)–C(9)	116.6 (9)

Table IV. Comparison of the Important Bond Lengths (Å) and Angles (deg) among $[W_2(O)_2(\mu\text{-}O)(\mu\text{-}S)(\mu\text{-edta})]^{2-}$, $[Mo_2(O)_2(\mu\text{-}O)(\mu\text{-}S)(\mu\text{-}R\text{-pdta})]^{2-}$,[24,a] and $[W_2(O)_2(\mu\text{-}O)_2(\mu\text{-edta})]^{2-}$[3]

	$[W_2O_3S(edta)]^{2-}$	$[Mo_2O_3S\text{-}(R\text{-pdta})]^{2-}$	$[W_2O_4(edta)]^{2-}$
M–M	2.6536 (6)	2.656 (1)	2.547 (7)
M–O(t)	1.792 (8)	1.68 (2)	1.74 (1)
M–S	2.348 (8)	2.32 (1)	
M–O(b)	1.904 (8)	1.945 (3)	1.93 (2)
M–O(l)	2.09 (2)	2.11 (1)	2.08 (2)
M–N	2.37 (2)	2.47 (6)	2.475 (3)
S–M–O(t)	103 (2)	105.8 (3)	
O(b)–M–O(t)	106 (2)	106.8 (6)	110.8
M–S–M	68.82 (8)	69.7 (1)	
M–O(b)–M	88.3 (4)	86.1 (2)	83.2
S–M–O(b)	99.0 (5)	98.7 (3)	
O(b)–M–O(b)			91.5
O(t)–M–O(l)	91.1 (9)	93 (2)	89.3
O(t)–M–N	161 (2)	159.7 (7)	

[a] *R*-pdta = (*R*)-propylenediaminetetraacetate(4–).

Table V. Electronic Absorption Spectral Data for $Na_2[W_2(O)_2(\mu\text{-}X)(\mu\text{-}Y)(\mu\text{-edta})]$ in Aqueous Solutions

X, Y	λ_{max}, nm (ϵ, M^{-1} cm^{-1})			
O, O	422 (380)	342 (1050)		276 (13 500)
O, S	440 (240)	342 (730)[a]	302 (4560)[a]	273 (9430)
S, S	449 (206)		305 (4710)[a]	273 (12 300)

[a] Shoulder.

structure.[25] Important bond lengths and angles of the present complex anion are compared in Table IV with those of $[Mo_2(O)_2(\mu\text{-}O)(\mu\text{-}S)(\mu\text{-}R\text{-pdta})]^{2-}$[26] (*R*-pdta = (*R*)-propylenediaminetetraacetate(4–)) and of $[W_2(O)_2(\mu\text{-}O)_2(\mu\text{-edta})]^{2-}$[3] in order to find the influence of metal ions and of bridging groups on the structure. The structural data for $[Mo_2(O)_2(\mu\text{-}O)(\mu\text{-}S)(\mu\text{-edta})]^{2-}$ are not available. Previous structural information on the $Mo_2(O)_2(\mu\text{-}S)_2$[24,26] and the $W_2(O)_2(\mu\text{-}O)_2$[3,27] complexes indicates that the edta and the pdta complexes have core structures very similar to each other; namely, bond distances and angles within the core are not significantly different from each other. Thus, the structural data for $[Mo_2(O)_2(\mu\text{-}O)(\mu\text{-}S)(\mu\text{-}R\text{-pdta})]^{2-}$[26] are given in Table IV. It is clear that the structural characteristics of $[W_2(O)_2(\mu\text{-}O)(\mu\text{-}S)(\mu\text{-edta})]^{2-}$ are very similar to those of $[Mo_2(O)_2(\mu\text{-}O)(\mu\text{-}S)(\mu\text{-}R\text{-pdta})]^{2-}$ and are appreciably different from those of $[W_2(O)_2(\mu\text{-}O)_2(\mu\text{-edta})]^{2-}$. Thus, the difference in metal ions, Mo or W, has only a small influence on the structure. Such a similarity has also been noted for $[M_2(O)_2(\mu\text{-}S)_2(\mu\text{-edta})]^{2-}$,[20,24] $[M_2(O)_2(\mu\text{-}S)_2(R\text{-cys})_2]^{2-}$ (*R*-cys = (*R*)-cysteinate(2–)),[6,28] and $[M_2(O)_2(\mu\text{-}O)_2(\mu\text{-}R\text{-pdta})]^{2-}$[26,27] (M = Mo, W).

2. Other Properties of $[W_2(O)_2(\mu\text{-}O)(\mu\text{-}S)(\mu\text{-edta})]^{2-}$. Other properties of the new complex $[W_2(O)_2(\mu\text{-}O)(\mu\text{-}S)(\mu\text{-edta})]^{2-}$ were studied in comparison with those of similar molybdenum and tungsten complexes with bridging oxide and sulfide, $[M_2(O)_2(\mu\text{-}X)(\mu\text{-}Y)(\mu\text{-edta})]^{2-}$ (M = Mo, W; X, Y = O, S).

(a) Electronic Absorption Spectrum. Figure 2 compares the absorption spectrum of the present complex with those of $[W_2(O)_2(\mu\text{-}O)_2(\mu\text{-edta})]^{2-}$ and $[W_2(O)_2(\mu\text{-}S)_2(\mu\text{-edta})]^{2-}$. Numerical absorption data are summarized in Table V. As noted previously for the dimolybdenum(V) complexes, a non-sulfur donor ligand such as edta does not give a strong charge-transfer band and transitions related to the core group are clearly seen.[29] $[W_2(O)_2(\mu\text{-}O)_2(\mu\text{-edta})]^{2-}$ has three bands at 422, 342, and 276 nm.[30] $[W_2(O)_2(\mu\text{-}O)(\mu\text{-}S)(\mu\text{-edta})]^{2-}$ has two distinctive bands at 440 and 273 nm, which may correspond to the first and the third band, respectively, of the bis(μ-oxo) complex. The bands at 449 and 273 nm of the bis(μ-sulfido) complex may also be assigned similarly. Distinctive shoulders at ca. 302 nm of the μ-oxo–μ-sulfido complex and at 305 nm of the bis(μ-sulfido) complex are more likely to be due to transitions characteristic of the sulfido-bridged complexes.

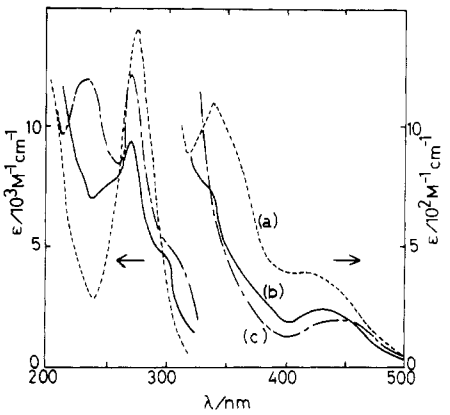

Figure 2. Electronic absorption spectra of $Na_2[W_2(O)_2(\mu\text{-}X)(\mu\text{-}Y)(\mu\text{-edta})]$ (X, Y = O, S) in aqueous solutions: (a) X = Y = O, (b) X = O, Y = S; (c) X = Y = S.

Table VI. Core Electron Binding Energies (eV) for the Complexes $Na_2[M_2(O)_2(\mu\text{-}X)(\mu\text{-}Y)(\mu\text{-edta})]$ (M = Mo, W; X, Y = O, S)[a]

complex (M_2XY)	Mo $3d_{3/2}$	Mo $3d_{5/2}$	W $4d_{3/2}$	W $4d_{5/2}$	W $4f_{5/2}$	W $4f_{7/2}$
Mo_2OO	234.7	231.5				
Mo_2OS	233.5	230.3				
Mo_2SS	233.5	230.3				
W_2OO			258.7	246.0	36.0	33.9
W_2OS			258.1	245.4	35.3	33.3
W_2SS			257.7	244.9	35.3	33.3

[a] Binding energies are calibrated for the C 1s peak (methylene part of $edta^{4-}$) at 284.6 eV.

Bands of the μ-sulfido complexes corresponding to that at 342 nm of the bis(μ-oxo) complex would become weaker in intensity and are masked by the stronger bands in the higher energy region. It seems that at least two of the three transitions of the bis(μ-oxo) complex do not significantly change their transition energies upon replacement of the oxide bridge by the sulfide one. A similar conclusion has been described for the series of the dimolybdate(V) complexes.[29] If the transitions are of common nature between the dimolybdate(V) and the ditungstate(V) complexes,[31] then the molecular orbital considerations of $[Mo_2(O)_2(\mu\text{-}O)_2(R\text{-cys})_2]^{2-}$ and other complexes[32-34] should be applied to the $W_2(O)_2(\mu\text{-}X)(\mu\text{-}Y)$ complexes. All the transitions discussed above would then be assigned to the transitions between the orbitals composed mainly of metal–metal interactions.

(b) X-ray Photoelectron Spectra. Binding energies of the Mo 3d and the W 4d and 4f electrons of the molybdenum and the tungsten dimers, respectively, with oxide and sulfide bridges are summarized in Table VI. There is an obvious trend that the binding energy decreases as the number of bridging sulfides increases. Interestingly, a similar trend was observed for the two complexes $W_2(O)_2(\mu\text{-}S)_2(S_2CNEt_2)_2$ and $W_2(S)_2(\mu\text{-}S)_2$-

(25) The N–C–C–N part of $[W_2(O)_2(\mu\text{-}O)_2(\mu\text{-edta})]^{2-}$ has been reported to have a planar conformation.[3b]
(26) Kojima, A.; Ooi, S.; Sasaki, Y.; Suzuki, K. Z.; Saito, K.; Kuroya, H. *Bull. Chem. Soc. Jpn.* **1981**, *54*, 2457–2465.
(27) Ikari, S.; Sasaki, Y.; Ito, T. To be submitted for publication.
(28) Brown, D. H.; Jeffreys, J. A. D. *J. Chem. Soc., Dalton Trans.* **1973**, 732–735.
(29) Suzuki, K. Z.; Sasaki, Y.; Ooi, S.; Saito, K. *Bull. Chem. Soc. Jpn.* **1980**, *53*, 1288–1298.
(30) These values are in reasonable agreement with those reported in ref 3a.
(31) The three bands of the $W_2(O)_2(\mu\text{-}O)_2$ complex are concluded to be similar to those of the $Mo_2(O)_2(\mu\text{-}O)_2$ complex from a comparison of the circular dichroism spectra of the *R*-pdta complexes of $W_2(O)_2(\mu\text{-}O)_2$ and $Mo_2(O)_2(\mu\text{-}O)_2$.[27]
(32) Brown, D. H.; Perkins, P. G.; Stewart, J. J. *J. Chem. Soc., Dalton Trans.* **1972**, 1105–1108.
(33) Brown, D. H.; Perkins, P. G. *Rev. Roum. Chim.* **1975**, *20*, 515–512.
(34) Jezowska-Trzebiatowska, B.; Glowiak, T.; Rudolf, M. F.; Sabat, M.; Sabat, J. *Russ. J. Inorg. Chem. (Engl. Transl.)* **1977**, *22*, 1590–1597.

Table VII. Peak Potentials (V vs SCE) of Reduction and Oxidation Processes for the Complexes $[M_2(O)_2(\mu\text{-}X)(\mu\text{-}Y)(\mu\text{-edta})]^{2-}$ (M = Mo, W; X, Y = O, S) in Aqueous Solution at pH = 7.5[a,b]

complex (M_2XY)	E_{pc}	E_{pa}	complex (M_2XY)	E_{pc}	E_{pa}
Mo_2OO	−1.32	+0.95	W_2OO	<−1.5	+0.43
Mo_2OS	−1.08	+1.14	W_2OS	<−1.5	+0.65
Mo_2SS	−1.02	+1.36	W_2SS	<−1.5	+0.98

[a] pH = 7.5 (0.015 M NaH_2PO_4, 0.185 M Na_2HPO_4, 0.182 M Na_2SO_4); [complex] = 0.001 M. [b] Glassy-carbon electrode; scan rate 20 mV s^{-1}.

$(S_2CNEt_2)_2$, in which the terminal ligands are replaced.[35] Such a trend has also been observed for the series of trinuclear molybdenum(IV) complexes $[Mo_3(\mu_3\text{-}X)(\mu\text{-}X)_3(NCS)_9]^{5-}$, where the four X species are combinations of oxide and sulfide ions.[36] The more electronegative oxygen makes the electron density of metal ions much less, resulting in higher binding energies.

(c) Electrochemistry. Reduction potentials of the three dimolybdenum(V) complexes in aqueous solution are known to be subject to pH dependence, more negative potentials occurring at higher pH.[18] In order to compare the redox behavior of the $M_2(O)_2(\mu\text{-}X)(\mu\text{-}Y)$ complexes, cyclic voltammograms were obtained at the fixed pH 7.5 (0.015 M NaH_2PO_4, 0.185 M Na_2HPO_4, 0.182 M Na_2SO_4) and at [complex] = 0.001 M. The redox potentials are summarized in Table VII. One oxidation wave was observed for all the molybdenum and the tungsten complexes within the range from −1.5 to +1.0 V vs SCE. A reduction process was not observed for the tungten complexes in the range studied. It is clear from Table VII that both oxidation and reduction potentials shift to the negative direction as the molybdenum ion is replaced by tungsten and to the positive direction as the bridging oxide is replaced by sulfide. Thus, molybdenum and bridging sulfide stabilize the reduced state more. The difference in redox potentials associated with the difference in the metal ion is understood by taking into account the higher electronegativity of molybdenum.[12] The trend observed for the difference in the bridging groups cannot be explained by the difference in electronegativity between oxygen and sulfur. It has been interpreted for the series of molybdenum dimers by considering a higher delocalization of metal orbitals due to the involvement of sulfur d orbitals, which makes the molecular orbitals (composed basically of the metal d orbitals) more stabilized.[18]

(d) ^1H and ^{13}C NMR Spectra. The ^1H NMR spectrum at 80 °C of $[W_2(O)_2(\mu\text{-}O)(\mu\text{-}S)(\mu\text{-edta})]^{2-}$ is shown in Figure 3 together with that of $[Mo_2(O)_2(\mu\text{-}O)(\mu\text{-}S)(\mu\text{-edta})]^{2-}$. If the edta ligand had a fixed pseudo-gauche conformation at the bridging N–C–C–N part as in the solid state of the ditungstate(V) complex (vide supra), all four acetate arms would be nonequivalent. The NMR spectra indicate that these complexes undergo conformational inversion in aqueous solution as observed for $[Mo_2(O)_2(\mu\text{-}O)_2(\mu\text{-edta})]^{2-}$.[37] The inversion is sufficiently rapid at 80 °C to show relatively simple NMR patterns. The acetate CH_2 part (at 3–4 ppm) of each of the two μ-O–μ-S complexes shows two AB patterns. Thus, two acetate groups on each side of the plane defined by O(t)–M–M–O(t) (M = Mo, W; O(t) = terminal oxide ion) should be equivalent. The signals are significantly broad at room temperature, as the inversion occurs at a rate just corresponding to the NMR time scale. The four ethylene protons that are in the two nonequivalent environments under the rapid inversion are observed as a singlet probably due to the small difference in chemical shift.

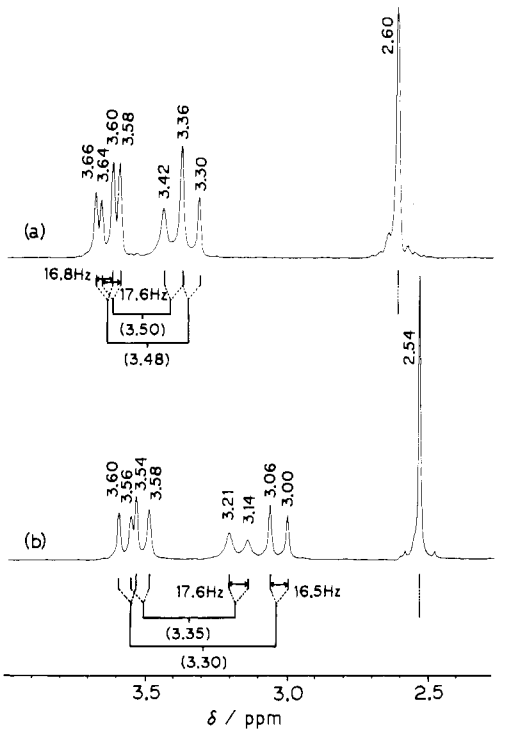

Figure 3. ^1H NMR spectra of $Na_2[M_2(O)_2(\mu\text{-}O)(\mu\text{-}S)(\mu\text{-edta})]$ in D_2O at 80 °C (δ = 0 for TSP ($(CH_3)_3Si(CD_2)_2COO^-Na^+$)): (a) M = W; (b) M = Mo. Arrows indicate coupling constants ($^2J_{H-H}$).

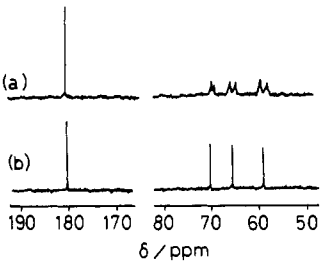

Figure 4. ^{13}C NMR spectra of $Na_2[W_2(O)_2(\mu\text{-}X)(\mu\text{-}Y)(\mu\text{-edta})]$ in D_2O (δ = 0 for DSS): (a) X = O, Y = S; (b) X = Y = S.

Figure 4a shows the ^{13}C NMR spectrum of $[W_2(O)_2(\mu\text{-}O)(\mu\text{-}S)(\mu\text{-edta})]^{2-}$, in which all the carbon signals are observed as broad peaks at room temperature, carbonyl C at 180.01, acetate C at 69.5, 68.8, 65.7, and 64.4, and ethylene C at 59.2 and 57.7 ppm. This spectrum is again understood by the inversion of the chelate ring. In contrast, $[W_2(O)_2(\mu\text{-}S)_2(\mu\text{-edta})]^{2-}$ shows sharp signals at room temperature at 180.90 (*C*=O), 69.90 and 65.28 (*C*H_2—CO), and 58.82 ppm (*C*H_2*C*H_2) (Figure 4b). Thus, the ligand conformation is fixed in this case. NMR spectra of a series of Mo^V and W^V dinuclear complexes indicate that the ligand conformational change is faster as the number of the oxide bridges increases. Quantitative analyses of the variable-temperature ^{13}C NMR spectra of a series of the complexes are in progress.[38]

Acknowledgment. We are grateful to Dr. Akira Nagasawa for the measurements and discussions of the NMR spectra and to Dr. Chizuko Kabuto for the crystal structure determination. The XPS spectra were obtained under a joint research program with the Institute for Molecular Science (1987–1988).

Supplementary Material Available: Table SI, listing anisotropic thermal parameters (1 page); Table SII, listing calculated and observed structure factors (9 pages). Ordering information is given on any current masthead page.

(35) Ansari, M. A.; Chandrasekaran, J.; Sarkar, S. *Bull. Chem. Soc. Jpn.* **1988**, *61*, 2265–2267.
(36) Shibahara, T.; Tsuru, H.; Kuroya, H. *Inorg. Chim. Acta* **1988**, *150*, 167–168.
(37) Blackmer, G. L.; Johnson, K. J.; Roberts, R. L. *Inorg. Chem.* **1976**, *15*, 596–601.
(38) Nagasawa, A.; Kamada, T.; Nakata, K.; Ikari, S.; Sasaki, Y.; Ito, T. Unpublished results.